Supporting Information

Ultrasensitive Photochromic and Raman Dual Response to Ethylenediamine Gas through Polyoxometalate-Viologen Crystalline Hybrid

Xi-Zhu Zhang,[a] Wen-Jing Zhu,[a] Zhong-Xi Yang,[a] Yi Feng,[a] Lin-Lin Fan,[a] Guang-Gang Gao*[a] and Hong Liu*[a]

[a] *School of Materials Science and Engineering, University of Jinan, Jinan, 250022, China.*

* *Corresponding author.*

E-mail: mse_gaogg@ujn.edu.cn (G.-G. Gao), mse_liuh@ujn.edu.cn (H. Liu)

Contents

Chemicals and materials

All chemicals and solvents obtained from suppliers were used without further purification. $K_6P_2W_{18}O_{62}\cdot 14H_2O$ (P_2W_{18}) and N, N'-bis(δ-aminopropyl)-4,4'-bipyridinium bromide hydrobromide (AV^{2+}) were prepared as described by published procedures.[1,2] Elem. Anal. calcd for $C_{16}H_{43}N_4O_{71.5}P_2W_{18}$: C, 3.99; H, 0.89; N, 1.17; W, 68.85%. Found: C, 3.93; H, 0.87; N, 1.08; W, 68.77%.

Characterization methods

Crystal data were collected on an Agilent Technology Eos Dual system with focusing multilayer mirror optics and a Cu Kα source of λ = 1.54184 Å. Data collection and reduction were performed using the program CrysAlisPro[3]. The intensities were corrected for absorption using the empirical method implemented in SCALE3 ABSPACK scaling algorithm. The structures were solved with intrinsic phasing methods (SHELXT-2015)[4], and refined by full-matrix least-squares on F^2 using OLEX2,[5] which utilizes the SHELXL-2015 module.[5] The positions of the metal atoms and their first coordination spheres were located from direct-methods. Other non-hydrogen atoms were found in alternating difference Fourier syntheses and least-squares refinement cycles. During the final cycles, except for some solvent molecules, all other non-hydrogen atoms were refined anisotropically. Hydrogen atoms were placed in calculated positions refined using idealized geometries and assigned fixed isotropic displacement parameters. The crystal structures are visualized by DIAMOND 3.2.[6] Crystallographic data of complex **1** was delivered to the

Cambridge Crystallographic Data Centre (CCDC) and assigned No. 2091528**.** Powder X-ray diffraction (PXRD) was performed using a D8 Discover (Bruker) diffractometer in Bragg-Brentano geometry (Cu Kα radiation, λ = 1.5418 Å). Data was recorded for the 2θ range from 5° to 80° in steps of 0.05° using an integration time of 1s. The FT-IR spectra were measured on a Nicolet 6700 spectrophotometer using KBr pellets in the range of 4000 to 500 cm^{-1}. UV-vis absorption spectra were measured in the reflectance mode at room temperature on a SHIMADZU UV-8000S spectrophotometer with an integrating sphere attachment and $BaSO_4$ as a reference. The X-ray photoelectron spectrum (XPS) was collected on an ESCA-LAB-MKII spectrometer (UK) to confirm the elemental composition and valence states. Transient photocurrent response tests were carried out using a CHI660E electrochemical workstation with a three-electrode system, in which a glassy carbon electrode was used as the working electrode, a platinum wire as the auxiliary electrode, and an Ag/AgCl electrode as the reference electrode. Raman test was performed using a Raman spectrometer (Labramis, Horiba Jobbin Yvon, Paris, France) with wavelength of 532 nm. The electron paramagnetic resonance spectrometer (EPR) was recorded at the X-band frequency (9.867 GHz) on a Bruker EMXplus-6/1spectrometer. Xenon lamp (300W 2.4 W cm^{-2}).

Raman and UV-vis detection

Various concentrations of ethylenediamine solution were obtained by continuously diluting the standard solution with ethanol. In the test experiment, crystals were first ground into powder and the fine powders with dispersing in

ethanol solution were drop-casted on the filtrate paper. In a clean and sealed conical flask, it was dropped into EDA solution, and then put the sample disc into the flask and seal it quickly, and then heated it to 60 °C for 4 hours to ensure complete volatilization of the gas. Finally, sample disc was pasted on a glass plate for detection by confocal Raman microscopy and UV-vis spectroscopy.

Photo-fatigue resistance

The complex 1 was irradiated by Xenon lamp for 10 minutes to become dark blue. Then, the sample after irradiation was heated at 80 °C for 15 minutes leading to the decoloration. Both the coloration and decoloration states can be detected by UV-vis spectra. Moreover, the maximum absorbance at 760 nm was selected for monitoring the coloration-decoloration cycles.

Supporting figures

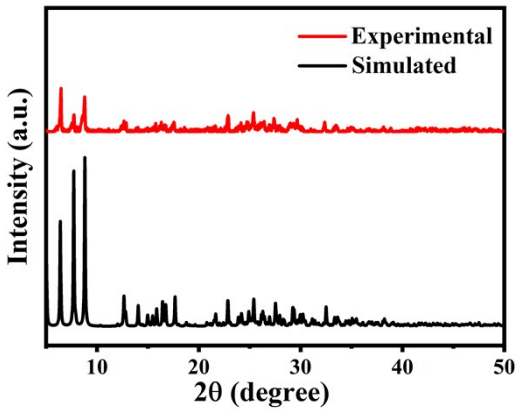

Fig. S1 Experimental and simulated PXRD patterns of complex **1**.

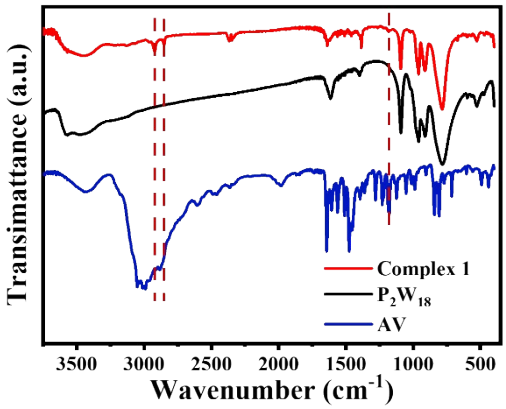

Fig. S2 FTIR spectra of complex **1**, P_2W_{18} and AV.

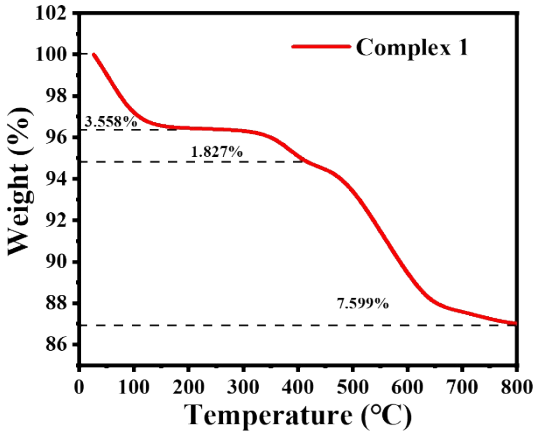

Fig. S3 TGA curve of complex **1** under N_2 atmosphere.

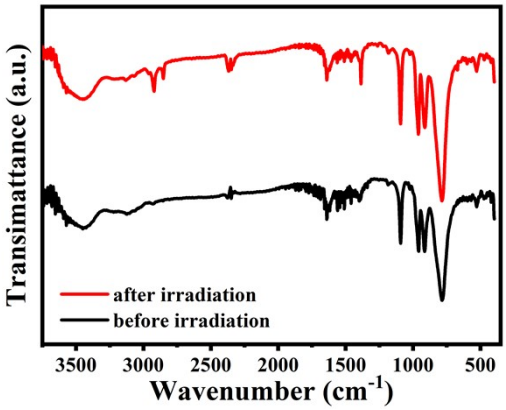

Fig. S4 FTIR spectra of complex **1** before and after ultraviolet light irradiation.

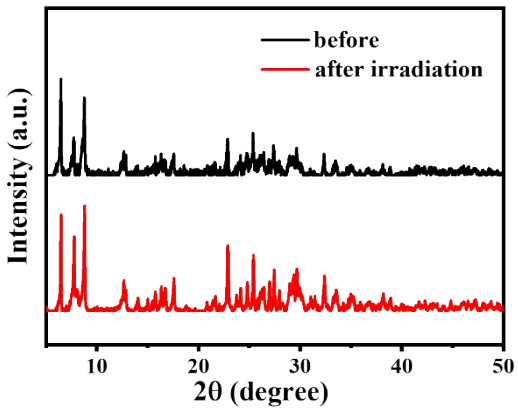

Fig. S5 PXRD patterns of complex **1** before and after ultraviolet light irradiation.

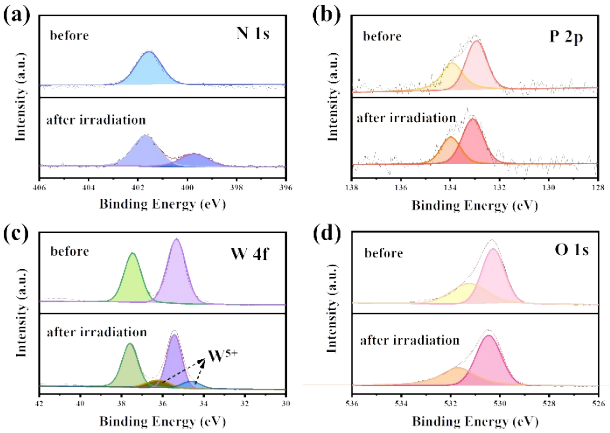

Fig. S6 XPS spectra of complex **1** before and after ultraviolet light irradiation: (a) N 1s, (b) P 2p, (c) W 4f and (d) O 1s.

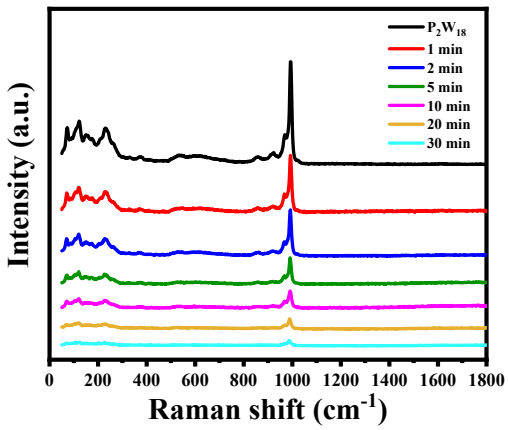

Fig. S7 Raman spectra of P_2W_{18} upon different irradiation time.

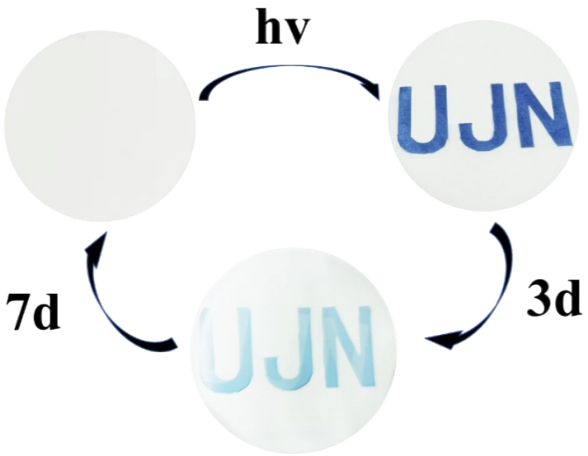

Fig. S8 Photograph of the photo-printed paper with a UJN motif and its bleaching after 3 and 7 days.

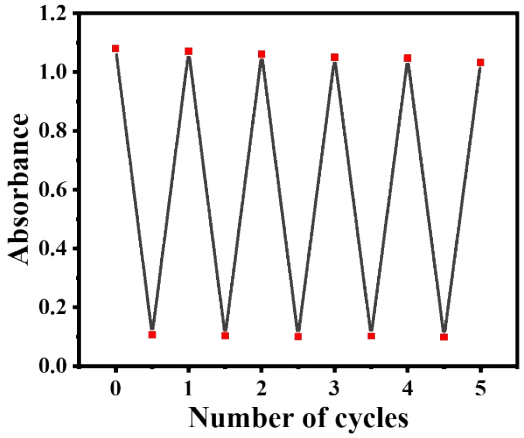

Fig. S9 The Number Cycles of photochromism.

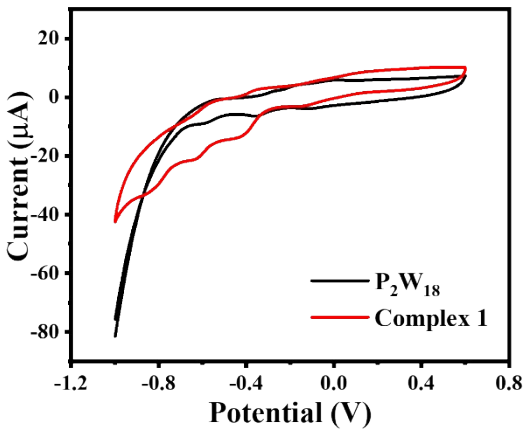

Fig. S10 Cyclic voltammogram of P_2W_{18} and complex **1** in 0.5 M H_2SO_4 aqueous solution.

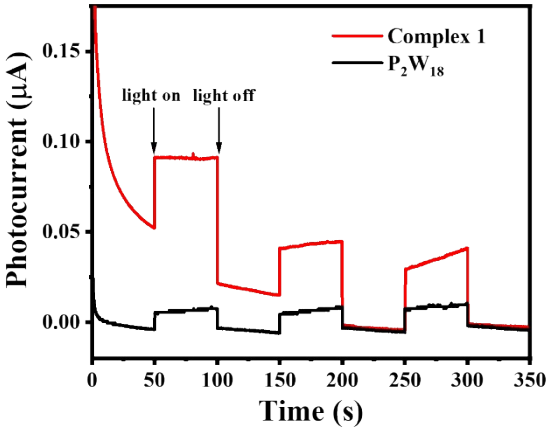

Fig. S11 Transient photocurrent responses of P_2W_{18} and complex **1** obtained with ultraviolet light at no constant bias in 0.5 M H_2SO_4 aqueous solution.

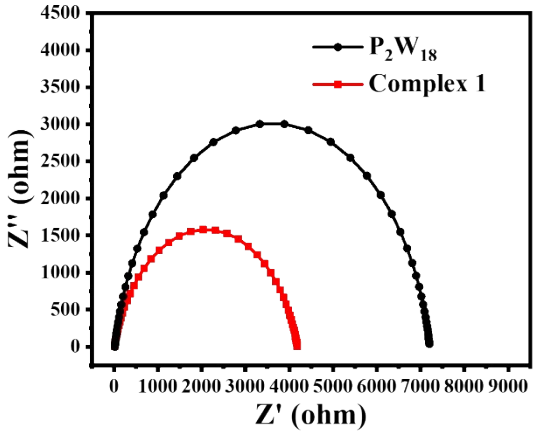

Fig. S12 Electrochemical impedance spectra (EIS) of P_2W_{18} and complex **1** at an overpotential of 200 mV.

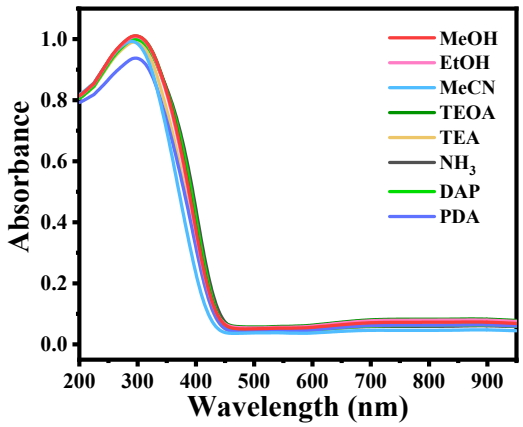

Fig. S13 UV-vis absorbance spectra of complex **1** after treatment with different solvents.

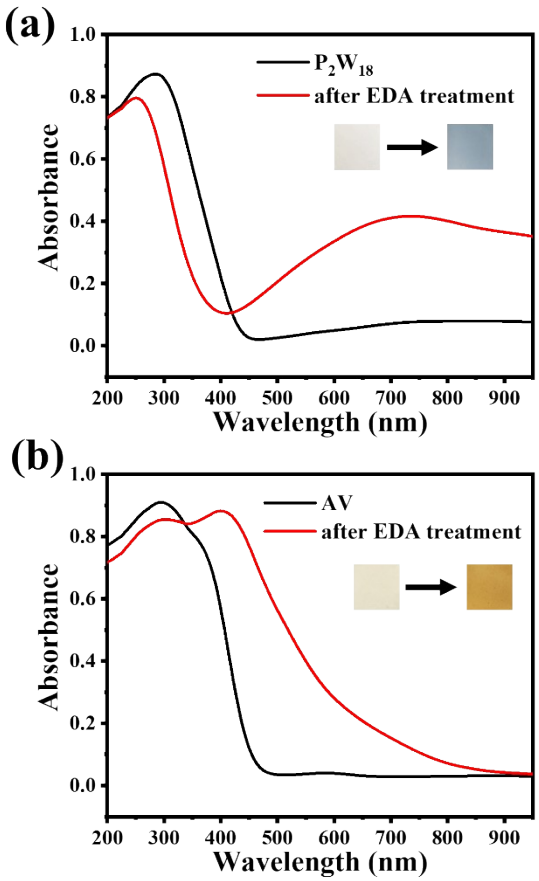

Fig. S14 Color changes and UV-vis absorbance spectra of P_2W_{18}(a) and AV(b) after treatment with EDA gas (30 ppm).

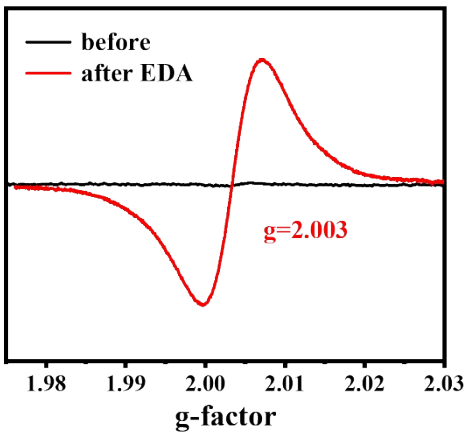

Fig. S15 ESR spectra of complex **1** before and after reaction with EDA gas.

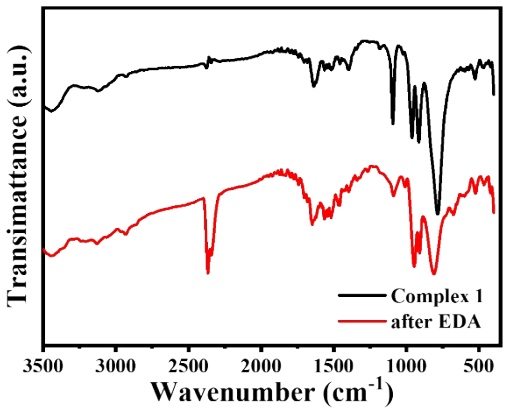

Fig. S16 FTIR spectra of complex **1** before and after reaction with EDA gas.

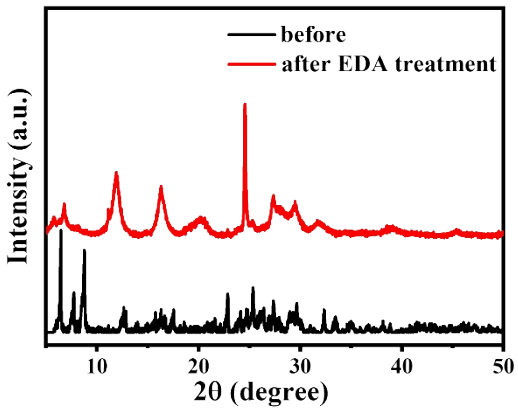

Fig. S17 PXRD patterns of complex **1** before and after reaction with EDA gas.

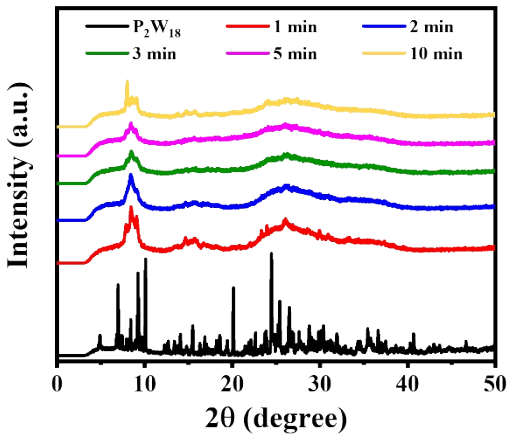

Fig. S18 PXRD patterns of P_2W_{18} upon different irradiation time.

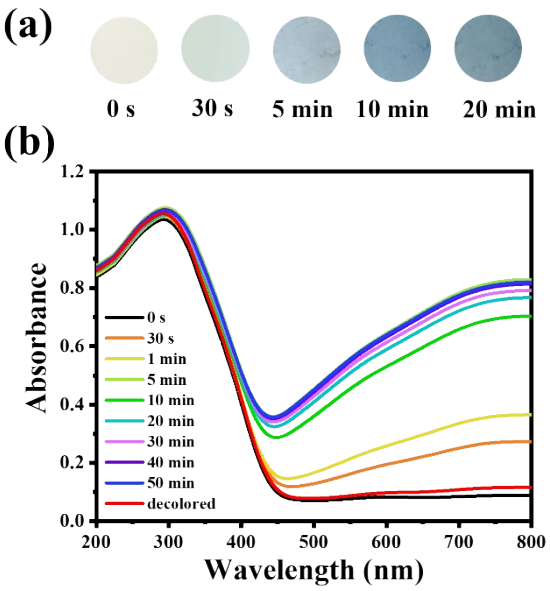

Fig. S19 Color changes (a) and UV-vis spectra (b) of **1** via different visible light (>400nm) irradiation time.

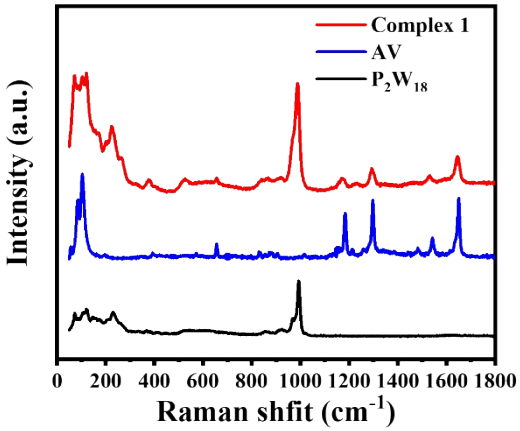

Fig. S20 Raman spectra of complex **1**, AV and P_2W_{18}.

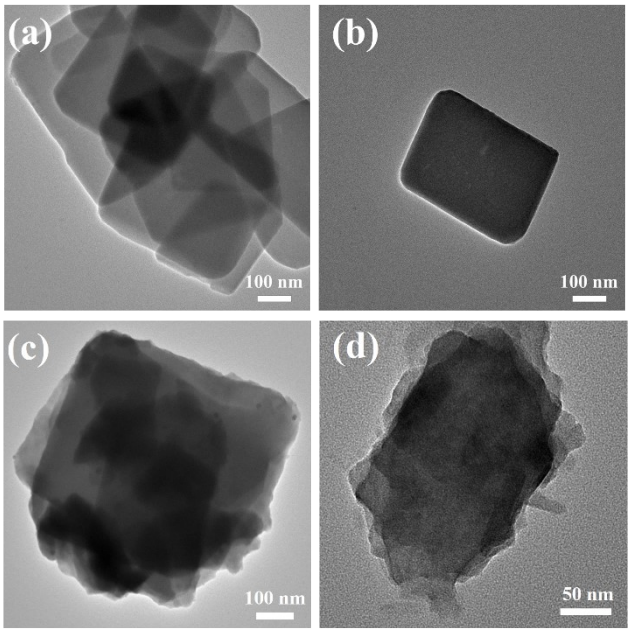

Fig. S21 TEM diagram of complex **1** before (a, b) and after irradiation (c) and after EDA treatment (d).

Table S1 Crystal Data and Structure Refinements for compound **1**

Empirical formula	$C_{16}H_{43}N_4O_{71.5}P_2W_{18}$
Formula weight	4806.06
Temperature /K	293(2)
Crystal system	Orthorhombic
Space group	*Pnna*
a / Å	12.2103(3)
b / Å	22.9104(4)
c / Å	27.6227(5)
α/ deg	90
β / deg	90
γ / deg	90
Volume / Å^3	7727.2(3)
Z	8
D_c / g cm^{-3}	4.000
F (000)	8064.0
Reflns collected / unique	23740/ 6821
$R_{(int)}$	0.0500
Goodness-of-fit on F^2	1.034
final *R* indices [I>2σ(I)]	R_1 = 0.0396 wR_2 = 0.0924
R indices (All data)	R_1 = 0.0477 wR_2 = 0.0956
Largest diff. peak / hole	1.66 e. Å^3/-1.97 e. Å^3

[a]$R_1 = \sum||F_o| - |F_c||/\sum|F_o|$, [b]$wR_2 = \{\sum w[(F_o)^2 - (F_c^2)]^2/\sum w[(F_o)^2]^2\}^{1/2}$.

Table S2 Selected bond lengths (Å) for complex **1**

Bond	Distance/Å	Bond	Distance/Å
W(3)-O(23)	1.889(8)	W(9)-O(15)1	1.928(9)
W(3)-O(24)[1]	1.955(8)	W(9)-O(21)	1.900(8)
W(3)-O(27)	1.915(8)	W(9)-O(24)	1.869(8)
W(3)-O(11)	2.361(8)	W(9)-O(31)1	1.924(8)
W(3)-O(33)	1.710(9)	W(9)-O(35)	1.737(8)
W(4)-O(22)	1.897(8)	W(9)-O(14)1	2.347(8)
W(4)-O(26)	1.939(8)	P(10)-O(12)	1.536(8)
W(4)-O(28)	1.903(8)	P(10)-O(11)	1.518(9)
W(4)-O(30)	1.726(9)	P(10)-O(13)	1.536(8)
W(4)-O(32)	1.888(8)	P(10)-O(14)	1.580(8)
W(4)-O(13)	2.343(8)	N(45)-C(46)	1.502(18)
W(5)-O(17)	1.917(9)	N(45)-C(44)	1.355(17)
W(5)-O(18)	1.912(8)	N(45)-C()50	1.355(16)
W(5)-O(27)1	1.898(8)	N(49)-C(48)	1.500(18)
W(5)-O(29)	1.891(9)	C(48)-C(47)	1.539(19)
W(5)-O(11)1	2.402(8)	C(47)-C(46)	1.51(2)
W(5)-O(36)	1.712(9)	C(51)-C(43)	1.414(17)
W(6)-O(23)	1.899(8)	C(51)-C(44)	1.35(2)
W(6)-O(25)	1.912(8)	C(43)-C(43)[2]	1.46(2)
W(6)-O(28)	1.912(8)	C(43)-C(42)	1.390(17)
W(6)-O(31)	1.895(8)	C(50)-C(42)	1.364(19)
W(6)-O(13)	2.374(8)		

Symmetry transformations used to generate equivalent atoms: [1]+X, 3/2-Y, 3/2-Z; [2]3/2-X, 1-Y, +Z

References

1 Christopher. R. G and Richard. G. F, *Inorg. Chem.*, 2008, **47**, 3679-3686.

2 M. S. Simon and P. T. Moore, *J. Polym. Sci. Pol. Chem.*, 1975, **13**, 1-16.

3 CrysAlisPro 2012, Agilent Technologies. Version 1.171.36.31.

4 G. M. Sheldrick, *Acta. Cryst. A*, 2015, **71**, 3-8.

5 O. V. Dolomanov, L. J. Bourhis, R. J. Gildea, J. A. K. Howard and H. Puschmann, *J. Appl. Cryst.*, 2009, **42**, 339-341.

6 K. Brandenburg, Diamond, 2010.